arXiv:1304.4776v1 [math.GN] 17 Apr 2013

BRAIDS, COMPLEX VOLUME, AND CLUSTER ALGEBRA

KAZUHIRO HIKAMI AND REI INOUE

Abstract. We give a cluster algebraic interpretation of complex volume of knots. Constructed is the R-operator in terms of the cluster mutations, and we clarify a correspondence between the cluster variables and the 3-dimensional hyperbolic geometry.

1. Introduction

Geometrical property of quantum invariants receives renewed interests since proposed is the volume conjecture [13, 17], which suggests a relationship between the colored Jones polynomial and the hyperbolic volume of knot complements. As quantum invariants of knots such as the colored Jones polynomial are constructed by use of the Artin braid relation, it is interesting to study a hyperbolic geometrical solution of the braid relation.

A fundamental object in the 3-dimensional hyperbolic geometry is an ideal tetrahedron, whose complex volume, *i.e.*, a complexification of hyperbolic volume, is written in terms of the extended Rogers dilogarithm function [20]. On the other hand, the cluster algebra has been developed recently since the pioneering work [6], and there exist many applications including representation theory, Teichmüller theory, integrable systems and so on. The dilogarithm function plays an important role also in the cluster algebra [4, 19].

Purpose of this article is to give a cluster algebraic interpretation of complex volume of knots. In our previous paper [9], we gave an interpretation of the cluster mutation as a hyperbolic ideal tetrahedron, and we proposed a method to compute the complex volume of 2-bridge knots. In this article, we construct the R-operator using the cluster mutation (Theorem 2.3), which can be geometrically regarded as a hyperbolic octahedron composed of four ideal tetrahedra. Via the R-operator, a knot with the braid group presentation is written in algebraic equations for cluster variables. Our main claim is Theorem 3.1, which gives a formula of complex volume in terms of cluster variables. Our construction can be naturally quantized with a help of the quantum cluster algebra [10].

This paper is organized as follows. In section 2, after explaining minimal basics of cluster algebra, we introduce the R-operator. In Section 3, we interpret the R-operator in hyperbolic geometry, and formulate the complex volume of knots at Theorem 3.1. Some examples of numerical calculation are presented in section 4.

Date: April 17, 2013.

2. Cluster Algebra and Braid Relation

2.1 Cluster Variable

We briefly introduce a notion of cluster algebra used in this article. A basic reference is [6].

A cluster seed $(\boldsymbol{x}, \mathbf{B})$ is a pair of

- a cluster variable $\boldsymbol{x} = (x_1, \dots, x_N)$: an N-tuple of algebraically independent variables,
- an exchange matrix $\mathbf{B} = (b_{ij})$: an $N \times N$ skew symmetric integer matrix.

For each $k = 1, \dots, N$, we define the mutation μ_k of $(\boldsymbol{x}, \mathbf{B})$ by

$$\mu_k\,(\boldsymbol{x}, \mathbf{B}) = (\widetilde{\boldsymbol{x}}, \widetilde{\mathbf{B}}), \tag{2.1}$$

where

- $\widetilde{\boldsymbol{x}} = (\widetilde{x}_1, \dots, \widetilde{x}_N)$ is
$$\widetilde{x}_i = \begin{cases} x_i, & \text{for } i \neq k, \\ \dfrac{1}{x_k} \left(\displaystyle\prod_{j: b_{jk} > 0} {x_j}^{b_{jk}} + \prod_{j: b_{jk} < 0} {x_j}^{-b_{jk}} \right), & \text{for } i = k, \end{cases} \tag{2.2}$$
- $\widetilde{\mathbf{B}} = (\widetilde{b}_{ij})$ is
$$\widetilde{b}_{ij} = \begin{cases} -b_{ij}, & \text{for } i = k \text{ or } j = k, \\ b_{ij} + \dfrac{|b_{ik}|\, b_{kj} + b_{ik}\, |b_{kj}|}{2}, & \text{otherwise.} \end{cases} \tag{2.3}$$

The pair $(\widetilde{\boldsymbol{x}}, \widetilde{\mathbf{B}})$ is again a cluster seed. We remark that the mutation μ_k is involutive, and that we have $\mu_j\, \mu_k(\boldsymbol{x}, \mathbf{B}) = \mu_k\, \mu_j(\boldsymbol{x}, \mathbf{B})$ if $b_{jk} = 0$.

In terms of the cluster variable $\boldsymbol{x}$, we introduce the y-variable, $\boldsymbol{y} = (y_1, \dots, y_N)$, defined by [7]

$$y_j = \prod_k {x_k}^{b_{kj}}. \tag{2.4}$$

The mutation μ_k acts on the y-variable as

$$\mu_k(\boldsymbol{y}, \mathbf{B}) = (\widetilde{\boldsymbol{y}}, \widetilde{\mathbf{B}}), \tag{2.5}$$

where $\widetilde{\mathbf{B}}$ is (2.3), and $\widetilde{\boldsymbol{y}} = (\widetilde{y}_1, \dots, \widetilde{y}_N)$ with $\widetilde{y}_j = \prod_k {\widetilde{x}_k}^{\widetilde{b}_{kj}}$ is given by

$$\widetilde{y}_i = \begin{cases} {y_k}^{-1}, & \text{for } i = k, \\ y_i\, \left(1 + {y_k}^{-1}\right)^{-b_{ki}}, & \text{for } i \neq k,\ b_{ki} \geq 0, \\ y_i\, (1 + y_k)^{-b_{ki}}, & \text{for } i \neq k,\ b_{ki} \leq 0. \end{cases} \tag{2.6}$$

2.2 R-operator

We set the exchange matrix $\mathbf{B}$ as

$$\mathbf{B}=\begin{pmatrix} 0 & 1 & -1 & 0 & 0 & 0 & 0 \\ -1 & 0 & 0 & 1 & 0 & 0 & 0 \\ 1 & 0 & 0 & -1 & 0 & 0 & 0 \\ 0 & -1 & 1 & 0 & 1 & -1 & 0 \\ 0 & 0 & 0 & -1 & 0 & 0 & 1 \\ 0 & 0 & 0 & 1 & 0 & 0 & -1 \\ 0 & 0 & 0 & 0 & -1 & 1 & 0 \end{pmatrix}. \tag{2.7}$$

By regarding the matrix element as

$$b_{ij}=\#\{\text{arrows from } i \text{ to } j\}-\#\{\text{arrows from } j \text{ to } i\}, \tag{2.8}$$

exchange matrix $\mathbf{B}$ corresponds to quiver, which is dual to triangulated surface (see, *e.g.*, [5]). In our case (2.7), we have the quiver and the triangulated surface depicted in Fig. 1.

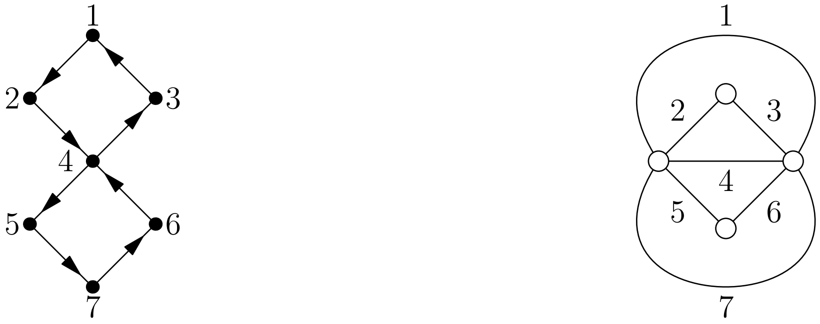

Figure 1. Quiver and triangulated surface

Definition 2.1. We define the R-operator by

$$\mathsf{R}=s_{3,5}\,s_{2,5}\,s_{3,6}\,\mu_4\,\mu_2\,\mu_6\,\mu_4. \tag{2.9}$$

Here we have used the permutation $s_{i,j}$ of subscripts i and j in seeds,

$$s_{i,j}(\dots,x_i,\dots,x_j,\dots)=(\dots,x_j,\dots,x_i,\dots).$$

Actions on the exchange matrix are defined in the same manner. Note that we have

$$\mathsf{R}^{-1}=s_{3,6}\,s_{2,5}\,s_{3,5}\,\mu_4\,\mu_5\,\mu_3\,\mu_4. \tag{2.10}$$

The permutations are included in the R-operator so that the exchange matrix $\mathbf{B}$ (2.7) is invariant under R. Explicitly we have

$$\mathsf{R}^{\pm1}(\boldsymbol{x},\mathbf{B})=(\mathsf{R}^{\pm1}(\boldsymbol{x}),\mathbf{B}), \tag{2.11}$$

where

$$\mathsf{R}(\boldsymbol{x}) = \begin{pmatrix} x_1 \\ x_5 \\ \dfrac{x_1\,x_3\,x_5 + x_3\,x_4\,x_5 + x_1\,x_2\,x_6}{x_2\,x_4} \\ \dfrac{x_1\,x_3\,x_4\,x_5 + x_3\,{x_4}^2\,x_5 + x_1\,x_3\,x_5\,x_7 + x_3\,x_4\,x_5\,x_7 + x_1\,x_2\,x_6\,x_7}{x_2\,x_4\,x_6} \\ \dfrac{x_3\,x_4\,x_5 + x_3\,x_5\,x_7 + x_2\,x_6\,x_7}{x_4\,x_6} \\ x_3 \\ x_7 \end{pmatrix}^{\top},$$

$$\mathsf{R}^{-1}(\boldsymbol{x}) = \begin{pmatrix} x_1 \\ \dfrac{x_1\,x_3\,x_5 + x_1\,x_2\,x_6 + x_2\,x_4\,x_6}{x_3\,x_4} \\ x_6 \\ \dfrac{x_1\,x_2\,x_4\,x_6 + x_2\,{x_4}^2\,x_6 + x_1\,x_3\,x_5\,x_7 + x_1\,x_2\,x_6\,x_7 + x_2\,x_4\,x_6\,x_7}{x_3\,x_4\,x_5} \\ x_2 \\ \dfrac{x_2\,x_4\,x_6 + x_3\,x_5\,x_7 + x_2\,x_6\,x_7}{x_4\,x_5} \\ x_7 \end{pmatrix}^{\top}. \qquad (2.12)$$

Correspondingly, actions of the R-operator, (2.9) and (2.10), on the y-variable are respectively given as follows:

$$\mathsf{R}(\boldsymbol{y}) = \begin{pmatrix} y_1\,(1 + y_2 + y_2 y_4) \\ \dfrac{y_2\,y_4\,y_5\,y_6}{1 + y_2 + y_6 + y_2\,y_6 + y_2\,y_4\,y_6} \\ \dfrac{1 + y_2 + y_6 + y_2\,y_6 + y_2\,y_4\,y_6}{y_2\,y_4} \\ \dfrac{y_4}{(1 + y_2 + y_2\,y_4)\,(1 + y_6 + y_4\,y_6)} \\ \dfrac{1 + y_2 + y_6 + y_2\,y_6 + y_2\,y_4\,y_6}{y_4\,y_6} \\ \dfrac{y_2\,y_3\,y_4\,y_6}{1 + y_2 + y_6 + y_2\,y_6 + y_2\,y_4\,y_6} \\ (1 + y_6 + y_4\,y_6)\,y_7 \end{pmatrix}^{\top},$$

$$\mathsf{R}^{-1}(\boldsymbol{y}) = \begin{pmatrix} \dfrac{y_1\, y_3\, y_4}{1+y_4+y_3\, y_4} \\ \dfrac{y_5}{1+y_4+y_3\, y_4+y_4\, y_5+y_3\, y_4\, y_5} \\ (1+y_4+y_3\, y_4+y_4\, y_5+y_3\, y_4\, y_5)\; y_6 \\ \dfrac{(1+y_4+y_3\, y_4)(1+y_4+y_4\, y_5)}{y_3\, y_4\, y_5} \\ y_2\; (1+y_4+y_3\, y_4+y_4\, y_5+y_3\, y_4\, y_5) \\ \dfrac{y_3}{1+y_4+y_3\, y_4+y_4\, y_5+y_3\, y_4\, y_5} \\ \dfrac{y_4\, y_5\, y_7}{1+y_4+y_4\, y_5} \end{pmatrix}^{\top} . \tag{2.13}$$

We remark that the R-operator (2.9) can be also written as

$$\mathsf{R} = s_{2,5}\, s_{3,6}\, \mu_2\, \mu_6\, \mu_4\, \mu_2\, \mu_6, \tag{2.14}$$

and that we have

$$s_{3,5}\ (\mu_3\, \mu_5\, \mu_4)^3 = 1,$$
$$s_{2,6}\ (\mu_2\, \mu_6\, \mu_4)^3 = 1.$$

2.3 Braid Relation

We generalize the quiver in Fig. 1 to that in Fig. 2. Therein also given is the triangulated surface, and an exchange matrix **B** is given by the rule (2.8) as a generalization of (2.7).

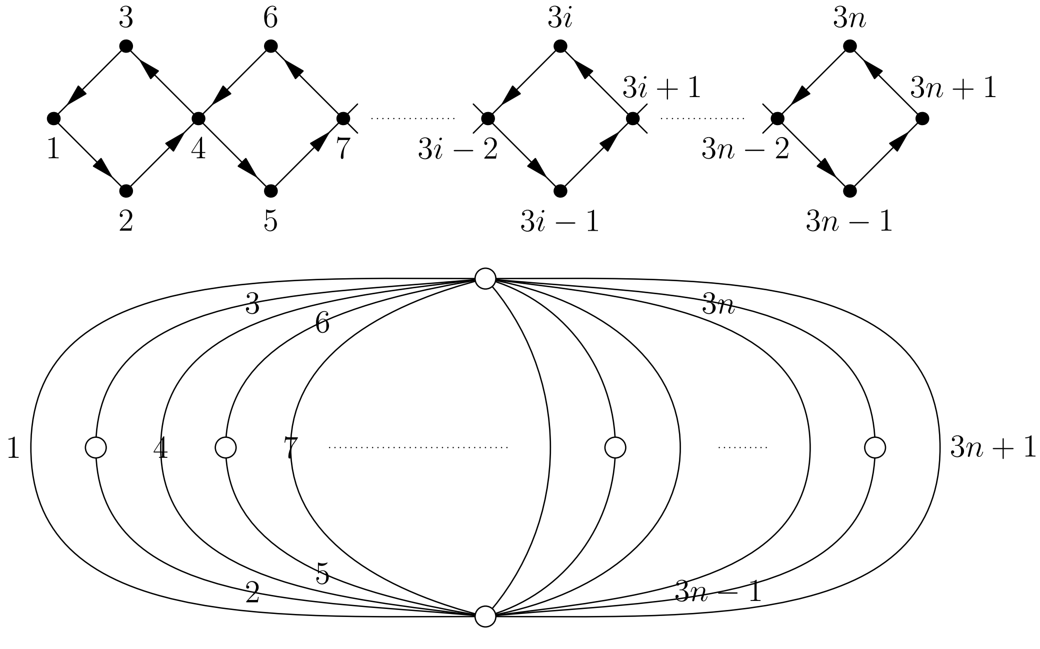

FIGURE 2. Quiver and triangulated surface.

Definition 2.2. By use of (2.9), we define the R-operator $\overset{i}{\mathsf{R}}$ for $i = 1, \ldots, n-1$ associated with the quiver in Fig. 2 by

$$\overset{i}{\mathsf{R}} = s_{3i,3i+2}\, s_{3i-1,3i+2}\, s_{3i,3i+3}\, \mu_{3i+1}\, \mu_{3i-1}\, \mu_{3i+3}\, \mu_{3i+1}. \tag{2.15}$$

Note that

$$\overset{i}{\mathsf{R}}{}^{-1} = s_{3i,3i+3}\, s_{3i-1,3i+2}\, s_{3i,3i+2}\, \mu_{3i+1}\, \mu_{3i+2}\, \mu_{3i}\, \mu_{3i+1}. \tag{2.16}$$

The exchange matrix associated to Fig. 2 is invariant under the action of the R-operators $\overset{i}{\mathsf{R}}{}^{\pm 1}$. The explicit forms of the actions on the cluster variable $\boldsymbol{x} = (x_1, x_2, \ldots, x_{3n+1})$ and the y-variable $\boldsymbol{y} = (y_1, y_2, \ldots, y_{3n+1})$ are as follows.

$$\overset{i}{\mathsf{R}}{}^{\pm 1}(\boldsymbol{x}) = \bigl(x_1, \ldots, x_{3i-3}, \mathsf{R}^{\pm 1}(x_{3i-2}, \ldots, x_{3i+4}), x_{3i+5}, \ldots, x_{3n+1}\bigr), \tag{2.17}$$

$$\overset{i}{\mathsf{R}}{}^{\pm 1}(\boldsymbol{y}) = \bigl(y_1, \ldots, y_{3i-3}, \mathsf{R}^{\pm 1}(y_{3i-2}, \ldots, y_{3i+4}), y_{3i+5}, \ldots, y_{3n+1}\bigr), \tag{2.18}$$

where $\mathsf{R}^{\pm 1}(x_1, \ldots, x_7)$ and $\mathsf{R}^{\pm 1}(y_1, \ldots, y_7)$ are defined in (2.12) and (2.13) respectively.

Theorem 2.3. *The* R*-operator satisfies the braid relation, namely we have*

$$\overset{i}{\mathsf{R}}\,\overset{i+1}{\mathsf{R}}\,\overset{i}{\mathsf{R}} = \overset{i+1}{\mathsf{R}}\,\overset{i}{\mathsf{R}}\,\overset{i+1}{\mathsf{R}}, \quad \textit{for } i = 1, 2, \ldots, n-2, \tag{2.19}$$

$$\overset{i}{\mathsf{R}}\overset{j}{\mathsf{R}} = \overset{j}{\mathsf{R}}\overset{i}{\mathsf{R}}, \quad \textit{for } |i-j| > 1. \tag{2.20}$$

Proof. The second equality is trivial.

It is sufficient to check $\overset{1}{\mathsf{R}}\overset{2}{\mathsf{R}}\overset{1}{\mathsf{R}} = \overset{2}{\mathsf{R}}\overset{1}{\mathsf{R}}\overset{2}{\mathsf{R}}$ on the cluster variable $(x_1, \ldots, x_{10})$ with the exchange matrix associated to Fig. 2 with $n = 3$. By direct computation, we can check that both actions, $\overset{1}{\mathsf{R}}\overset{2}{\mathsf{R}}\overset{1}{\mathsf{R}}$ and $\overset{2}{\mathsf{R}}\overset{1}{\mathsf{R}}\overset{2}{\mathsf{R}}$, result in the following same expressions,

$$\begin{aligned}
&\Biggl(x_1, x_8, \frac{x_1x_2x_4x_6x_8 + x_1x_3x_5x_7x_8 + x_3x_4x_5x_7x_8 + x_1x_2x_6x_7x_8 + x_1x_2x_4x_5x_9}{x_2x_4x_5x_7}, \\
&\frac{1}{x_2x_4x_5x_7x_9} \bigl(x_1x_2x_4x_6x_7x_8 + x_1x_3x_5{x_7}^2x_8 + x_3x_4x_5{x_7}^2x_8 + x_1x_2x_6{x_7}^2x_8 + x_1x_2x_4x_6x_8x_{10} \\
&\qquad + x_1x_3x_5x_7x_8x_{10} + x_3x_4x_5x_7x_8x_{10} + x_1x_2x_6x_7x_8x_{10} + x_1x_2x_4x_5x_9x_{10} \bigr), \\
&\qquad \frac{x_6x_7x_8 + x_6x_8x_{10} + x_5x_9x_{10}}{x_7x_9}, \frac{x_1x_3x_5 + x_3x_4x_5 + x_1x_2x_6}{x_2x_4}, \\
&\frac{1}{x_2x_4x_6x_7x_9} \bigl(x_1x_3x_4x_6x_7x_8 + x_3{x_4}^2x_6x_7x_8 + x_1x_3x_4x_6x_8x_{10} + x_3{x_4}^2x_6x_8x_{10} + x_1x_3x_4x_5x_9x_{10} \\
&\qquad + x_3{x_4}^2x_5x_9x_{10} + x_1x_3x_5x_7x_9x_{10} + x_3x_4x_5x_7x_9x_{10} + x_1x_2x_6x_7x_9x_{10} \bigr), \\
&\quad \frac{x_3x_4x_6x_7x_8 + x_3x_4x_6x_8x_{10} + x_3x_4x_5x_9x_{10} + x_3x_5x_7x_9x_{10} + x_2x_6x_7x_9x_{10}}{x_4x_6x_7x_9}, x_3, x_{10} \Biggr).
\end{aligned}$$

Actions on the y-variables are induced from these actions.

This completes the proof. □

See also [14], where used is a similar construction of solution of the Yang–Baxter equation.

3. Hyperbolic Geometry

3.1 Ideal Tetrahedron

A building block of hyperbolic 3-manifold is an ideal tetrahedron whose vertices are on the boundary of a hyperbolic 3-space [22]. An ideal hyperbolic tetrahedron $\triangle$ is parameterized with cross-ratio $z \in \mathbb{C}$ of its four vertices, and the volume of $\triangle$ is given by the Bloch–Wigner function,

$$D(z) = \Im \operatorname{Li}_2(z) + \arg(1-z) \log|z| \,. \tag{3.1}$$

As depicted in Fig. 3, opposite edges have the same dihedral angles. Therein we have used notations,

$$z' = 1 - \frac{1}{z}, \qquad\qquad z'' = \frac{1}{1-z}. \tag{3.2}$$

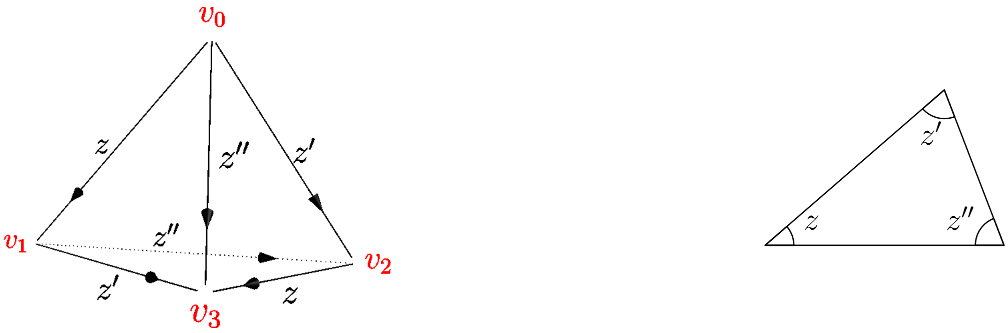

FIGURE 3. An oriented ideal tetrahedron (left), and a triangle as intersection with horosphere (right).

In case that a set of ideal tetrahedra $\{\triangle_\nu\}$ is glued faces together to a hyperbolic manifold $M = \bigcup_\nu \triangle_\nu$, the volume of M is given by

$$\operatorname{Vol}(M) = \sum_\nu D(z_\nu). \tag{3.3}$$

A complexification of $\operatorname{Vol}(M)$ known as a complex volume is defined with the Chern-Simons invariant $\operatorname{CS}(M)$. We have [20]

$$\mathrm{i}\left(\operatorname{Vol}(M) + \mathrm{i}\operatorname{CS}(M)\right) = \sum_\nu \operatorname{sgn}(\triangle_\nu)\ \mathrm{L}\left([z_\nu; p_\nu, q_\nu]\right), \tag{3.4}$$

where $[z_\nu; p_\nu, q_\nu]$ is an element of the extended Bloch group with integers p_ν and q_ν, and $\operatorname{sgn}(\triangle_\nu)$ is $+1$ (resp. -1) when the vertex ordering of $\triangle_\nu$ is same (resp. inverse) with Fig. 3. We have used the extended Rogers dilogarithm function

$$\mathrm{L}\left([z;p,q]\right) = \operatorname{Li}_2(z) + \frac{1}{2}\log z \log(1-z) + \frac{\pi\,\mathrm{i}}{2}\left(q \log z + p\log(1-z)\right) - \frac{\pi^2}{6}. \tag{3.5}$$

A method to compute p_ν and q_ν was proposed in [25]. For an oriented ideal tetrahedron of modulus z in Fig. 3, let c_{ab} be complex parameters on edge connecting vertices v_a and v_b. Assume that they fulfill

$$\frac{c_{03}\,c_{12}}{c_{02}\,c_{13}} = \pm z, \qquad \frac{c_{01}\,c_{23}}{c_{03}\,c_{12}} = \pm\left(1-\frac{1}{z}\right), \qquad \frac{c_{02}\,c_{13}}{c_{01}\,c_{23}} = \pm\frac{1}{1-z}. \tag{3.6}$$

Note that, in gluing tetrahedra together, identical edges have the same complex parameter. Then $[z; p, q]$, integers p and q for modulus z, is given by

$$\begin{aligned} \log z + p\,\pi\,\mathrm{i} &= \log c_{03} + \log c_{12} - \log c_{02} - \log c_{13}, \\ -\log(1-z) + q\,\pi\,\mathrm{i} &= \log c_{02} + \log c_{13} - \log c_{01} - \log c_{23}. \end{aligned} \tag{3.7}$$

3.2 Octahedron

In our previous paper [9], we demonstrated that the cluster mutation can be regarded as an attachment of ideal tetrahedron to triangulated surface (see also [18]). Furthermore we claimed that the cluster variable $\boldsymbol{x}$ corresponds to Zickert's complex parameters c_{ab} on edges.

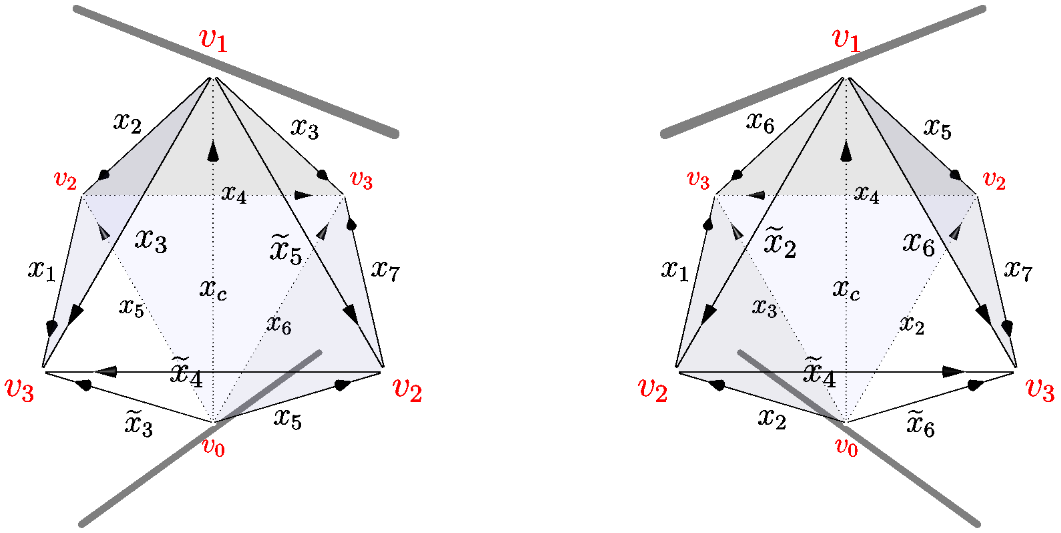

FIGURE 4. Octahedron for R (left) and R^{-1} (right)

Based on this observation, we see that the R-operator (2.9) is realized as an octahedron in Fig. 4, which is composed of four tetrahedra $\{\triangle_N, \triangle_S, \triangle_W, \triangle_E\}$. The four tetrahedra originate from four mutations in the R-operator, (2.9) and (2.10). In octahedra, the cluster variables x_k and $\widetilde{x}_k$ defined by

$$\widetilde{\boldsymbol{x}} = \mathsf{R}^{\pm 1}(\boldsymbol{x}),$$

are assigned to edges, and we have used

$$x_c = \frac{x_2\,x_6 + x_3\,x_5}{x_4}. \tag{3.8}$$

Note that we have fixed vertex ordering for our convention, and that edges with the same complex parameters (*e.g.*, two pairs of edges v_0–v_2, v_1–v_3) are identical.

As the R-operator satisfies the braid relation (Theorem 2.3), we can interpret that each octahedron is assigned to every crossing of knot diagram as in Fig. 5. This reminds a fact [21] that octahedron was assigned to the Kashaev R-matrix [12] (see also, [1, 3, 8, 16, 23]). Note that another expression (2.14) of the same R-operator corresponds to a decomposition of octahedron into five tetrahedra, which was used in studies of the colored Jones R-matrix at root of unity [2, 21].

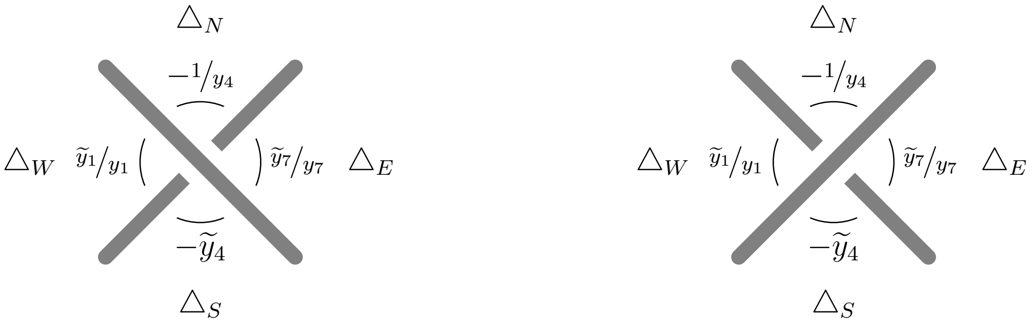

FIGURE 5. Dihedral angle at crossings, R (left) and R^{-1} (right).

		R			R^{-1}		
$\triangle$	Volume	$\operatorname{sgn}(\triangle)$	$z_\triangle$	$\dfrac{1}{1-z_\triangle}$	$\operatorname{sgn}(\triangle)$	$z_\triangle$	$\dfrac{1}{1-z_\triangle}$
$\triangle_N$	$D\left(-\dfrac{1}{y_4}\right)$	$-$	$-\dfrac{x_2\,x_6}{x_3\,x_5}$	$\dfrac{x_3\,x_5}{x_4\,x_c}$	$+$	$-\dfrac{x_3\,x_5}{x_2\,x_6}$	$\dfrac{x_2\,x_6}{x_4\,x_c}$
$\triangle_S$	$D\left(-\widetilde{y}_4\right)$	$-$	$-\dfrac{\widetilde{x}_3\,\widetilde{x}_5}{x_3\,x_5}$	$\dfrac{x_3\,x_5}{\widetilde{x}_4\,x_c}$	$+$	$-\dfrac{\widetilde{x}_2\,\widetilde{x}_6}{x_2\,x_6}$	$\dfrac{x_2\,x_6}{x_c\,\widetilde{x}_4}$
$\triangle_W$	$D\left(\dfrac{\widetilde{y}_1}{y_1}\right)$	$+$	$\dfrac{x_2\,\widetilde{x}_3}{x_3\,x_5}$	$-\dfrac{x_3\,x_5}{x_1\,x_c}$	$-$	$\dfrac{\widetilde{x}_2\,x_3}{x_2\,x_6}$	$-\dfrac{x_2\,x_6}{x_1\,x_c}$
$\triangle_E$	$D\left(\dfrac{\widetilde{y}_7}{y_7}\right)$	$+$	$\dfrac{\widetilde{x}_5\,x_6}{x_3\,x_5}$	$-\dfrac{x_3\,x_5}{x_c\,x_7}$	$-$	$\dfrac{x_5\,\widetilde{x}_6}{x_2\,x_6}$	$-\dfrac{x_2\,x_6}{x_c\,x_7}$

TABLE 1. Moduli of four tetrahedra assigned to operators R and R^{-1}. Sgn "+" (resp. "−") means that vertex ordering of tetrahedron is same (resp. inverse) with Fig. 3.

Taking into account of the vertex ordering of tetrahedra, we can determine moduli of each tetrahedron from (3.6) as in Table 1. From these results, we define dilogarithm functions for every crossing by

$$\mathrm{L}([\mathsf{R}^{\pm 1}]) = \sum_{t\in\{N,S,W,E\}} \operatorname{sgn}(\triangle_t)\ \mathrm{L}\left([z_{\triangle_t}; p_{\triangle_t}, q_{\triangle_t}]\right). \tag{3.9}$$

Here integers $p_{\triangle_t}$ and $q_{\triangle_t}$ are given from (3.7) by use of Table 1. For instance, $p_{\triangle_E}$ and $q_{\triangle_E}$ in the operator R are given as

$$p_{\triangle_E}\,\pi\,\mathrm{i} = -\log\left(\frac{\widetilde{x}_5\,x_6}{x_3\,x_5}\right) + \log(\widetilde{x}_5) + \log(x_6) - \log(x_3) - \log(x_5),$$

$$q_{\triangle_E}\,\pi\,\mathrm{i} = -\log\left(-\frac{x_3\,x_5}{x_c\,x_7}\right) + \log(x_3) + \log(x_5) - \log(x_c) - \log(x_7).$$

It should be remarked that, to identify the R-operator with a hyperbolic octahedron, we need a consistency condition around a central edge labeled by x_c in Fig. 4. This condition is automatically satisfied by

$$y_1\,y_4\,y_7 = \widetilde{y}_1\,\widetilde{y}_4\,\widetilde{y}_7,$$

where $\widetilde{\boldsymbol{y}} = \mathsf{R}^{\pm 1}(\boldsymbol{y})$ (2.13). In Fig. 5 denoted are dihedral angles around central axis assigned to each crossing.

3.3 Braid Group Presentation and Gluing Conditions

Our main claim is the following.

Theorem 3.1. *Let knot K have a braid group presentation $\sigma_{k_1}^{\varepsilon_1}\sigma_{k_2}^{\varepsilon_2}\cdots\sigma_{k_m}^{\varepsilon_m}$, where $\varepsilon_j = \pm 1$ and*

$$\mathcal{B}_n = \left\langle \sigma_1, \sigma_2, \dots, \sigma_{n-1} \;\middle|\; \begin{array}{c} \sigma_i\sigma_j = \sigma_j\sigma_i \text{ for } |i-j|>1 \\ \sigma_i\sigma_{i+1}\sigma_i = \sigma_{i+1}\sigma_i\sigma_{i+1} \text{ for } i = 1, 2, \dots, n-2 \end{array} \right\rangle .$$

We define a cluster pattern for $\boldsymbol{x}[j] = (x[j]_1, \dots, x[j]_{3n+1})$ by

$$\boldsymbol{x}[1] \xrightarrow{\overset{k_1}{\mathsf{R}}{}^{\varepsilon_1}} \boldsymbol{x}[2] \xrightarrow{\overset{k_2}{\mathsf{R}}{}^{\varepsilon_2}} \cdots \xrightarrow{\overset{k_m}{\mathsf{R}}{}^{\varepsilon_m}} \boldsymbol{x}[m+1], \tag{3.10}$$

with the exchange matrix associated to Fig. 2. We assume that the initial cluster variable $\boldsymbol{x}[1]$ satisfies

$$\boldsymbol{x}[1] = \boldsymbol{x}[m+1]. \tag{3.11}$$

Then there exist an algebraic solution of (3.11) *such that the complex volume of K is given by*

$$\mathrm{i}\left(\mathrm{Vol}(S^3 \setminus K) + \mathrm{i}\,\mathrm{CS}(S^3 \setminus K)\right) = \sum_{j=1}^{m} \mathrm{L}([\overset{k_j}{\mathsf{R}}{}^{\varepsilon_j}]). \tag{3.12}$$

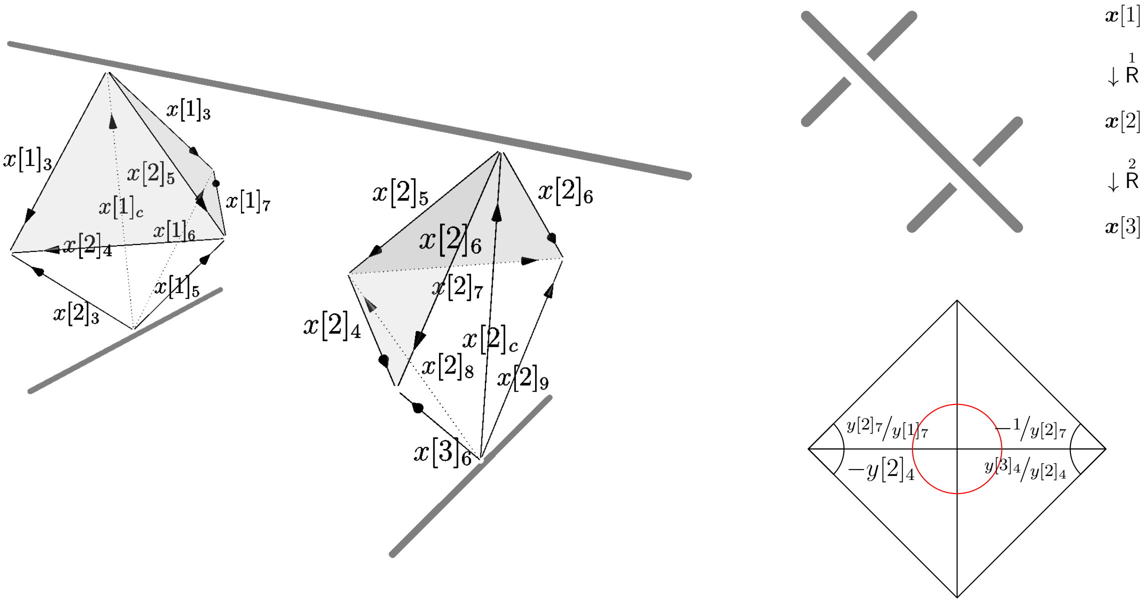

FIGURE 6. Gluing of octahedra (left) assigned to crossing (right top), and a developing map (right bottom). A consistency condition is read from a red circle.

To prove this theorem, we need to check consistency condition as [1, 8].

We have already seen that a consistency condition around a central axis of octahedra is fulfilled. We shall check other cases. First we study a cluster pattern

$$\boldsymbol{x}[1] \overset{\overset{1}{\mathsf{R}}}{\to} \boldsymbol{x}[2] \overset{\overset{2}{\mathsf{R}}}{\to} \boldsymbol{x}[3].$$

For each crossing we assign octahedra as in Fig. 6. Therein colored faces are glued together so that identical edges have the same complex parameters. Note that (2.12) implies $x[2]_6 = x[1]_3$ and $x[1]_7 = x[2]_7$, and that

$$x[1]_c = \frac{x[1]_2\, x[1]_6 + x[1]_3\, x[1]_5}{x[1]_4}, \qquad x[2]_c = \frac{x[2]_5\, x[2]_9 + x[2]_6\, x[2]_8}{x[2]_7}.$$

Consistency condition around edge labeled by complex parameter $x[2]_5$ is checked as

$$\frac{1}{1-\frac{y[2]_7}{y[1]_7}} \cdot \left(1+\frac{1}{y[2]_4}\right) \cdot (1+y[2]_7) \cdot \frac{1}{1-\frac{y[3]_4}{y[2]_4}} = 1.$$

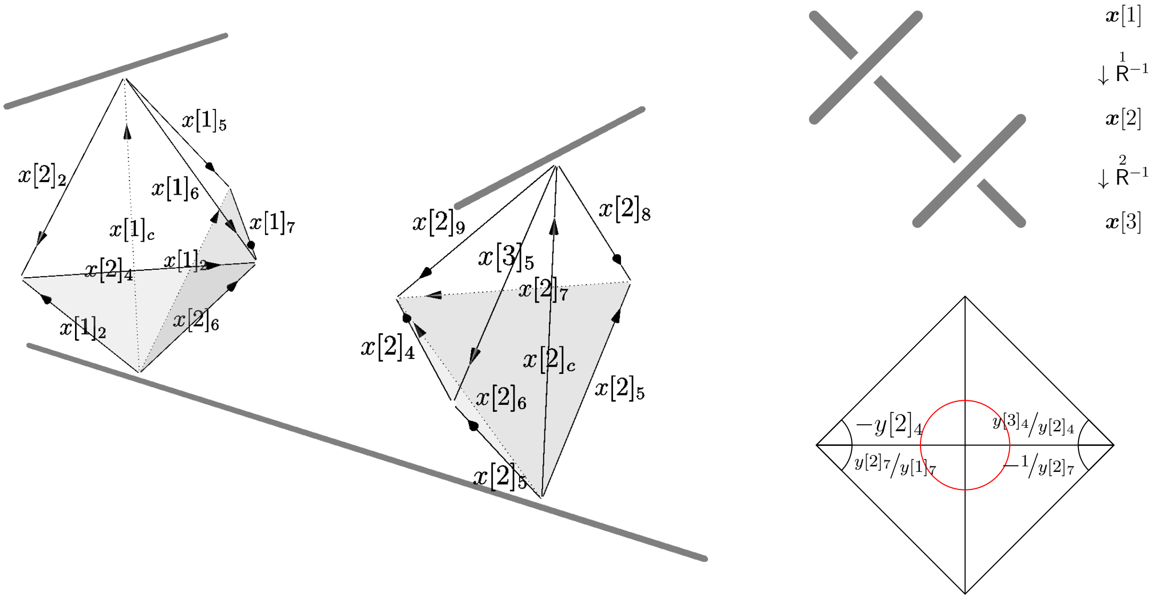

Figure 7. Gluing of octahedra (left) assigned to crossing (right top), and a developing map (right bottom). A consistency condition is read from a red circle.

Same is a case of a cluster pattern

$$\boldsymbol{x}[1] \xrightarrow{\overset{1}{\mathsf{R}}{}^{-1}} \boldsymbol{x}[2] \xrightarrow{\overset{2}{\mathsf{R}}{}^{-1}} \boldsymbol{x}[3].$$

We have octahedra as in Fig. 7, and we can check a consistency condition in the developing map as

$$\left(1-\frac{y[1]_7}{y[2]_7}\right) \cdot \frac{1}{1+y[2]_4} \cdot \left(1-\frac{y[2]_4}{y[3]_4}\right) \cdot \frac{1}{1+\frac{1}{y[2]_7}} = 1.$$

A completeness condition follows from alternating crossings. In the case that the cluster pattern is given by

$$\boldsymbol{x}[1] \xrightarrow{\overset{1}{\mathsf{R}}} \boldsymbol{x}[2] \xrightarrow{\overset{2}{\mathsf{R}}{}^{-1}} \boldsymbol{x}[3],$$

octahedra are attached to each crossing as in Fig. 8. See that identical edges have same complex parameters $x[2]_6 = x[1]_3$ and $x[1]_7 = x[2]_7$ due to (2.12). Then we can check the completeness condition as

$$\begin{aligned} \frac{1+\frac{1}{y[2]_4}}{1-\frac{y[2]_7}{y[1]_7}} \cdot \frac{1+\frac{1}{y[2]_7}}{1-\frac{y[2]_4}{y[3]_4}} &= y[1]_2\, y[1]_3 \\ &= 1. \end{aligned}$$

Here the last equality follows from (2.4).

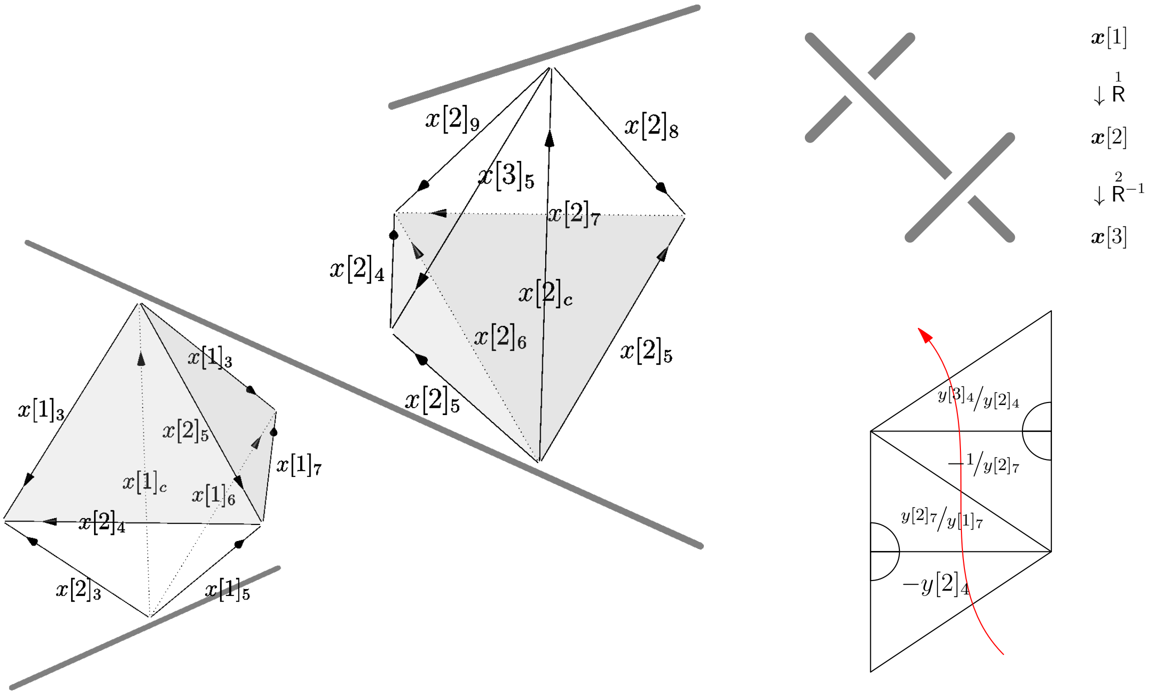

Figure 8. Gluing of octahedra (left) assigned to crossing (right top), and a developing map (right bottom). A completeness condition is read from a red curve.

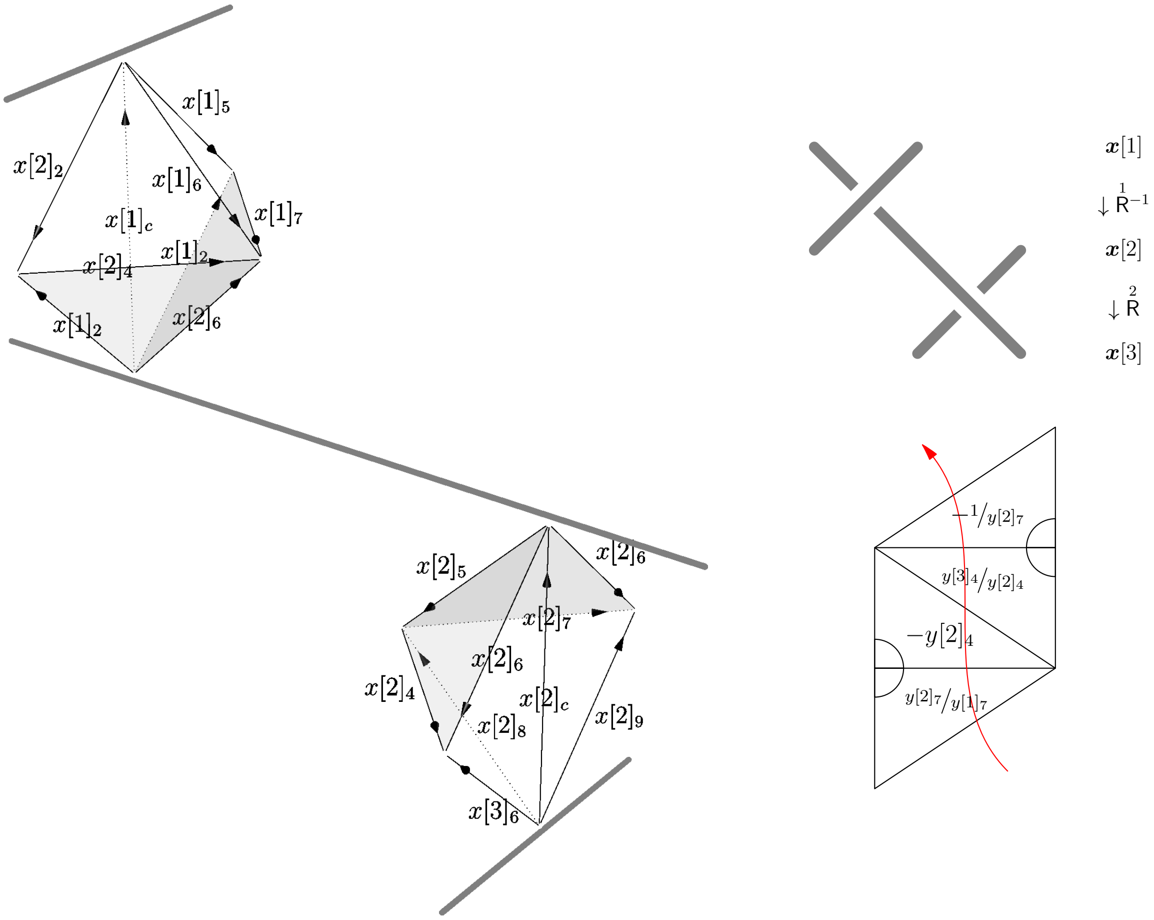

Figure 9. Gluing of octahedra (left) assigned to crossing (right top), and a developing map (right bottom).

We have Fig. 9 for a cluster pattern

$$\boldsymbol{x}[1] \xrightarrow{\overset{1}{\mathsf{R}^{-1}}} \boldsymbol{x}[2] \overset{\overset{2}{\mathsf{R}}}{\to} \boldsymbol{x}[3].$$

By use of (2.4), we have a completeness condition

$$\begin{aligned} \frac{1-\frac{y[1]_7}{y[2]_7}}{1+y[2]_4} \cdot \frac{1-\frac{y[3]_4}{y[2]_4}}{1+y[2]_7} &= y[1]_2\, y[1]_3 \\ &= 1. \end{aligned}$$

Other cases can be checked in a similar manner, and we can conclude that the R-operator is interpreted as a hyperbolic octahedron as in Fig. 4. This fact supports (3.12), and completes a proof.

We should note that the completeness condition is endowed from

$$y[1]_{3i-1}\, y[1]_{3i} = 1, \quad \text{for } i = 1, 2, \dots, n. \tag{3.13}$$

4. Examples

4.1 Figure-eight knot 4_1

We study the figure-eight knot whose braid group presentation is $\sigma_1 {\sigma_2}^{-1} \sigma_1 {\sigma_2}^{-1}$. The cluster pattern for 4_1 is thus

$$\boldsymbol{x}[1] \overset{\overset{1}{\mathsf{R}}}{\to} \boldsymbol{x}[2] \xrightarrow{\overset{2}{\mathsf{R}^{-1}}} \boldsymbol{x}[3] \overset{\overset{1}{\mathsf{R}}}{\to} \boldsymbol{x}[4] \xrightarrow{\overset{2}{\mathsf{R}^{-1}}} \boldsymbol{x}[5].$$

We can check that $\boldsymbol{x}[1] = \boldsymbol{x}[5]$ is fulfilled by, for example,

$$\boldsymbol{x}[1] = \left(x_1, x_2, x_2, 1, x_1\, x_2, {x_1}^2\, x_2, x_1, -x_2, -x_2, 1\right),$$

where $(x_1, x_2) = (\mathrm{e}^{2\pi \mathrm{i}/3}, 0)$. To compute the complex volume of 4_1, we set $(x_1, x_2) = (\mathrm{e}^{2\pi \mathrm{i}/3} + \delta, \delta)$ with $\delta \in \mathbb{R}_{>0}$, and take a limit $\delta \to 0$ at the last. We have checked numerically that (3.12) gives $\mathrm{i} \cdot 2\, D(\mathrm{e}^{\pi \mathrm{i}/3}) = \mathrm{i} \cdot 2.02988 \cdots$ as desired [22].

4.2 Trefoil knot 3_1

We observe that Theorem 3.1 can be also applied to the trefoil knot 3_1, which is not hyperbolic. The braid group presentation for 3_1 is ${\sigma_1}^3$, and its cluster pattern is

$$\boldsymbol{x}[1] \overset{\overset{1}{\mathsf{R}}}{\to} \boldsymbol{x}[2] \overset{\overset{1}{\mathsf{R}}}{\to} \boldsymbol{x}[3] \overset{\overset{1}{\mathsf{R}}}{\to} \boldsymbol{x}[4].$$

We solve $\boldsymbol{x}[1] = \boldsymbol{x}[4]$ by choosing an initial cluster variable as

$$\boldsymbol{x}[1] = (1, x, -x, 1, -x^2, 1, 1), \tag{4.1}$$

and get $x = \frac{1 \pm \mathrm{i}\sqrt{15}}{4}$. We check numerically that (3.12) gives $-8.22467 \cdots \simeq -\frac{5}{6}\pi^2$. It agrees with the Chern-Simons invariant of 3_1, which is also given from asymptotic limit of the Kashaev invariant [11, 15, 24].

Acknowledgments

The authors would like to thank Jun Murakami for stimulating discussions and for comments on the manuscript. The work of KH is supported in part by JSPS KAKENHI

Grant Number 23340115, 24654041. The work of RI is partially supported by JSPS KAKENHI Grant Number 22740111.

References

[1] J. Cho, H. Kim, and S. Kim, *Optimistic limits of Kashaev invariants and complex volumes of hyperbolic links*, preprint (2013), `arXiv:1301.6219 [math.GT]`.

[2] J. Cho and J. Murakami, *The complex volumes of twist knots via colored Jones polynomials*, J. Knot Theory Ramifications **19**, 1401–1421 (2010).

[3] J. Cho, J. Murakami, and Y. Yokota, *The complex volumes of twist knots*, Proc. Amer. Math. Soc. **137**, 3533–3541 (2009).

[4] V. V. Fock and A. B. Goncharov, *Cluster ensembles, quantization and the dilogarithm*, Ann. Sci. Éc. Norm. Supér. (4) **42**, 865–930 (2009), `math.AG/0311245`.

[5] S. Fomin, M. Shapiro, and D. Thurston, *Cluster algebras and triangulated surfaces I. cluster complexes*, Acta Math. **201**, 83–146 (2008), `math/0608367`.

[6] S. Fomin and A. Zelevinsky, *Cluster algebras I. foundations*, J. Amer. Math. Soc. **15**, 497–529 (2002), `arXiv:math/0104151`.

[7] ———, *Cluster algebras IV: coefficients*, Composito Math. **143**, 112–164 (2007), `arXiv:math/0602259`.

[8] K. Hikami, *Hyperbolic structure arising from a knot invariant*, Int. J. Mod. Phys. A **16**, 3309–3333 (2001), `arXiv:math-ph/0105039`.

[9] K. Hikami and R. Inoue, *Cluster algebra and complex volume of once-punctured torus bundles and two-bridge knots*, preprint (2012), `arXiv:1212.6042 [math.GT]`.

[10] ———, in preparation.

[11] K. Hikami and A. N. Kirillov, *Torus knot and minimal model*, Phys. Lett. B **575**, 343–348 (2003), `arXiv:hep-th/0308152`.

[12] R. M. Kashaev, *A link invariant from quantum dilogarithm*, Mod. Phys. Lett. A **10**, 1409–1418 (1995), `arXiv:q-alg/9504020`.

[13] ———, *The hyperbolic volume of knots from quantum dilogarithm*, Lett. Math. Phys. **39**, 269–275 (1997), `arXiv:q-alg/9601025`.

[14] ———, *On the spectrum of Dehn twists in quantum Teichmüller theory*, in A. N. Kirillov and N. Liskova, eds., *Physics and Combinatorics — Proceedings of the Nagoya 2000 International Workshop*, pp. 63–81, World Scientific, Singapore, 2001, `arXiv:math/0008148`.

[15] R. M. Kashaev and O. Tirkkonen, *Proof of the volume conjecture for torus knots*, Zap. Nauch. Sem. POMI **269**, 262–268 (2000), `arXiv:math/9912210`.

[16] H. Murakami, *Kashaev's invariant and the volume of a hyperbolic knot after Yokota*, in A. N. Kirillov, A. Tsuchiya, and H. Umemura, eds., *Physics and Combinatorics*, pp. 244–272, World Scientific, Singapore, 2001, proceedings of the Nagoya 1999 International Workshop, `arXiv:math/0008027`.

[17] H. Murakami and J. Murakami, *The colored Jones polynomials and the simplicial volume of a knot*, Acta Math. **186**, 85–104 (2001), `arXiv:math/9905075`.

[18] K. Nagao, Y. Terashima, and M. Yamazaki, *Hyperbolic geometry and cluster algebra*, preprint (2011), `arXiv:1112.3106 [math.GT]`.

[19] T. Nakanishi, *Periodicities in cluster algebras and dilogarithm identities*, in A. Skowronski and K. Yamagata, eds., *Representations of Algebras and Related Topics*, pp. 407–444, EMS Series of Congress Reports, European Mathematical Society (2011), `arXiv:1006.0632 [math.QA]`.

[20] W. D. Neumann, *Extended Bloch group and the Cheeger–Chern–Simons class*, Geom. Topol. **8**, 413–474 (2004), `arXiv:math/0307092 [math.GT]`.

[21] D. Thurston, *Hyperbolic volume and the Jones polynomial*, Lecture notes of École d'été de Mathématiques 'Invariants de nœuds et de variétés de dimension 3', Institut Fourier (1999).

[22] W. P. Thurston, *The geometry and topology of three-manifolds*, Lecture Notes in Princeton University, Princeton (1980).

[23] Y. Yokota, *On the complex volume of hyperbolic knots*, J. Knot Theory Ramifications **20**, 955–976 (2011).

[24] D. Zagier, *Vassiliev invariants and a strange identity related to the Dedekind eta-function*, Topology **40**, 945–960 (2001).

[25] C. K. Zickert, *The volume and Chern–Simons invariant of a representation*, Duke Math. J. **150**, 489–532 (2009), `arXiv:0710.2049 [math.GT]`.

Faculty of Mathematics, Kyushu University, Fukuoka 819-0395, Japan.

E-mail address: `KHikami@gmail.com`

Department of Mathematics and Informations, Faculty of Science, Chiba University, Chiba 263-8522, Japan.

E-mail address: `reiiy@math.chiba-u.ac.jp`